Perpendicular Lamellae in Parallel Lamellae in a Hierarchical CECEC-P Hexablock Terpolymer

Guillaume Fleury and Frank S. Bates*

Department of Chemical Engineering and Materials Science, University of Minnesota, Minneapolis, Minnesota 55455

Received November 21, 2008

ABSTRACT: We describe the synthesis and phase behavior of a nearly monodisperse poly(cyclohexylethylene-*b*-ethylene-*b*-cyclohexylethylene-*b*-ethylene-*b*-cyclohexylethylene-*b*-ethylene-*alt*-propylene) (CECEC-P) hexablock terpolymer, synthesized by sequential anionic polymerization followed by catalytic hydrogenation. This multiblock copolymer, which contains equal volume fractions of P and compositionally symmetric CECEC, microphase separates through chemical incompatibility between C, E, and P and exhibits a complex morphology with two different length scales related to the local (C-E) and overall (C-E-P) sequences. We have identified a perpendicular lamellae in parallel lamellae mesostructure in the CECEC-P sample, where layers of rubbery P separate sheets of alternating layers of semicrystalline E and glassy C, arranged perpendicular to the larger overall lamellar structure.

Introduction

Virtually every field of science, engineering, and technology relies on the creation of structure at multiple length scales for the production of useful devices.[1] A ubiquitous theme is the rational design of morphology beginning with molecular synthesis and finishing with the processing of a final product. Metal alloys, semiconductor devices, drug delivery vehicles, and dialysis membranes all rely on the precise arrangement of materials into functional configurations. Aside from biological systems, which benefit from evolutionary optimization, block copolymers offer some of the most spectacular examples of exquisite structure at a macromolecular scale. While the principles of block copolymer self-assembly[2−4] have been recognized for more than half a century, relatively few products, and only a handful of molecular architectures, have penetrated the marketplace, most notably SBS and SIS triblock-based thermoplastic elastomers and $(SB)_n$ multiblock thermoplastics.[5−7] Yet, modern synthetic methods offer an unlimited array of block configurations containing two, three, or more monomeric constituents, which can be arrayed in linear,[8−11] branched,[12] graft,[10,13,14] and other molecular configurations.[15−18] This unbounded design freedom is both a benefit and a bane since the relationships that dictate morphology and ultimately applications have not been extended beyond rather simple two-monomer systems.

We have been exploring the design of multiblock copolymers[19−21] for several years with the objective of combining multiple functions (e.g., mechanical toughness, optical clarity, ionic conductivity) in single-component materials based on commercially viable monomers. Fully saturated systems derived from styrene, butadiene, and isoprene are particularly attractive since they combine three basic physical ingredients: glass (poly(cyclohexylethylene (C)), semicrystal (poly(ethylene) (E)), and rubber (poly(ethylene-*alt*-propylene) (P)). Our intention is to configure these polymers into minimally complex molecular architectures while achieving a specific morphology. One of our targets is a lamellar morphology that contains a substructure of lamellae arranged perpendicular to the larger layered structure. We believe this new arrangement will yield superior mechanical properties and may offer opportunities in the development of advanced membranes.

* To whom correspondence should be addressed. E-mail: bates@cems.umn.

Matsushita and co-workers[22−25] have prepared related hierarchical lamellar morphologies from S′ISISISISIS′[22] and VISISISISIV[23] undecablock copolymers where S, I, and V refer to poly(styrene), poly(isoprene), and poly(2-vinylpyridine), respectively. (We have changed the author's notation from P to V to avoid confusion with our convention in referring to poly(ethylene-*alt*-propylene).) Two types of parallel lamellae were induced by creating an asymmetric architecture with $M_{n,S'} \approx 5M_{n,S}$ and $M_{n,V} \approx 5M_{n,S}$ with $M_{n,S} \approx M_{n,I}$. Striking TEM images reveal two periodicities, d_1 and d_2, in these materials, a short one determined by the core ISISISISI segments and a larger one established by the nanoblock sequence and the large S′ and V end blocks. Matsushita et al. demonstrate that either molecular weight asymmetry (S vs S′) or chemical dissimilarity (V vs S and I) can lead to this type of doubly periodic parallel lamellar state. Our goal in this work was to produce a related but different arrangement, where layers with a shorter period are arranged perpendicular to the ones with the longer repeat spacing.

Experimental Section

A SBSBS-I hexablock copolymer was prepared by the sequential polymerization of styrene, butadiene, and isoprene in cyclohexane at 40 °C initiated by *sec*-butyllithium.[26] Subsequent catalytic hydrogenation was performed over a platinum/rhenium catalyst supported on a porous silica substrate, provided by the Dow Chemical Co.[27] Characterization by ^{1}H NMR confirmed >98% saturation and the target (25%/25%/50%) composition. An overall number-average molecular weight of $M_n = 120$ kg/mol and polydispersity $M_w/M_n = 1.09$ were established by a combination of gel permeation chromatography and ^{1}H NMR.[28]

Dynamic mechanical spectroscopy analysis using a Rheometrics Scientific ARES strain-controlled rheometer indicated that the order−disorder transition temperature for this material is greater than 300 °C. The glass transition temperature of the C blocks ($T_{g,C}$) was associated with the maximum in an isochronal tan(δ) measurements ($\omega = 1$ rad/s) obtained while heating and cooling between 110 and 150 °C. Virtually identical peak tan(δ) were recorded while heating and cooling.

Differential scanning calorimetry (TA Instruments Q1000 DSC) was employed with heating and cooling rates of 10 °C/min to determine the glass transition temperature of the P block ($T_{g,P}$) and melting ($T_{m,E}$) and crystallization ($T_{c,E}$) temperatures of the E blocks. Specimens were heated to and held at 200 °C for 10 min prior to measurement to minimize the effects of processing history.

10.1021/ma900060f CCC: $40.75
Published on Web 02/10/2009

Small-angle X-ray scattering patterns were obtained from the CECEC-P specimen at various temperatures between 140 and 250 °C at the Argonne National Laboratory using the equipment maintained by the DuPont−Northwestern−Dow Collaborative Access Team (DND-CAT). An X-ray wavelength (λ) of 1.032 Å with a sample-to-detector distance of 2.01 m was employed, and scattered X-ray intensity was recorded on an area detector and reduced to the one-dimension form of intensity vs scattering wavevector magnitude $q = 4\pi\lambda^{-1}\sin(\theta/2)$ where θ is the scattering angle.

TEM images of the multiblock copolymer were acquired using a JEOL 1210 transmission electron microscope operating at 120 kV in the bright field mode. Samples were prepared and stained according to established procedures.[30] Briefly, samples were cryomicrotomed at −120 °C using a diamond knife to create a flat surface and then stained by exposure to ruthenium tetroxide vapors to create contrast between different microdomains. Stained thin sections (60−90 nm) were then produced by again microtoming at −120 °C for subsequent TEM analysis.

Results and Discussion

We targeted a CECEC-P hexablock copolymer containing equal volume fractions of E (25%) and C (25%) and equal amounts of CECEC and P (50%) for this study, i.e., compositionally symmetric on two length scales. Lamellar forming CECEC pentablocks are mechanically sound[29] while a P domain comprised of singly tethered chains should permit shear alignment or layer separation (e.g., by swelling with solvent). Figure 1a illustrates a representative SAXS result obtained at 140 °C. Four reflections are evident, which cannot be indexed according to a single conventional morphology such as lamellae or hexagonally packed cylinders. However, the three highest q peaks occur with spacings q^*, $2q^*$, and $3q^*$, as would be expected for a periodic layered morphology. The lowest q peak is not related to this sequence in a sensible way. Similar SAXS patterns were obtained at the other measurement temperatures as shown in Figure 1b for $T = 250$ °C, which allow us to exclude segregation induced by the crystallization of the E blocks and confirm a single doubly periodic ordered state at elevated temperatures between $T_{g,C} \approx 125$ °C (see below) and 300 °C.

This observation is strengthened by the thermal analyses for the CECEC-P terpolymer depicted in Figure 2. The glass transition of the C blocks ($T_{g,C} \approx 125$ °C) occurs at a significantly higher temperature than the melting ($T_{m,E} \approx 90$ °C) or crystallization ($T_{c,E} \approx 60$ °C) temperatures of the E blocks, i.e., about 65 °C higher than the point of crystallization during cooling. Thus, vitrification of the C domains will inhibit reorganization of the melt morphology when the E blocks crystallize.

In order to better understand the morphology responsible for the SAXS results, we investigated the CECEC-P multiblock copolymer using transmission electron microscopy (TEM). Figure 3 shows one of many images recorded from a thin section (ca. 70 nm) of the material obtained after staining with ruthenium tetroxide (RuO_4). In previous publications[29,30] we have shown that this heavy metal stain is preferentially absorbed by rubbery P domains followed by C domains and then E domains in saturated hydrocarbon block copolymers. Thus, we interpret the gray scale contrast in Figure 3 as deriving from layers of P (darkest contrast) sequenced with layers of C (lighter gray) and E (white) that are arranged perpendicular to the P layers. This hierarchical structure is consistent with the interpretation of two length scales, $d_1 = 59$ nm and $d_2 = 23$ nm, that emerged from the SAXS data.

Combining the SAXS and TEM evidence, we arrive at the morphological assignment illustrated in Figure 4, where layers of rubbery P separate sheets of alternating layers of semicrystalline E and glassy C, arranged perpendicular to the larger overall lamellar structure. This microdomain organization differs qualitatively from the fully parallel version shown by Matsushita et al. We can rationalize this interesting arrangement based on the documented sequence of segment−segment interaction parameters that govern C, E, and P: $\chi_{CE}(T) > \chi_{CP}(T) \gg \chi_{EP}(T)$.[31−33] Therefore, on enthalpic grounds E-P contacts are most favored and C-E are energetically most costly. However, the sequence of blocks in CECEC-P mandates both C-E and C-P interfaces within any fully (i.e., three domains) microphase-separated structure. The perpendicular structure shown in Figure 4 replaces a fraction of these higher energy surfaces with low energy E-P interfaces, thus lowering the overall free energy. This argument accounts for the qualitative difference between the CECEC-P morphology denoted "perpendicular lamellae in parallel lamellae" and Matsushita's doubly parallel lamellae for VISISISISIV, where $\chi_{VI} > \chi_{VS} \approx \chi_{IS}$.

Entropically this morphology may be optimal as well. Space filling at constant density dictates the ratio d_1/d_2 in either the perpendicular or parallel forms. We estimate that CECEC-P would form three stripes (C, E, and C) separated by one P domain if packed in the doubly parallel lamellar form. A CECEC pentablock copolymer can assume six possible configurations in a one-dimensional lamellar lattice ranging from

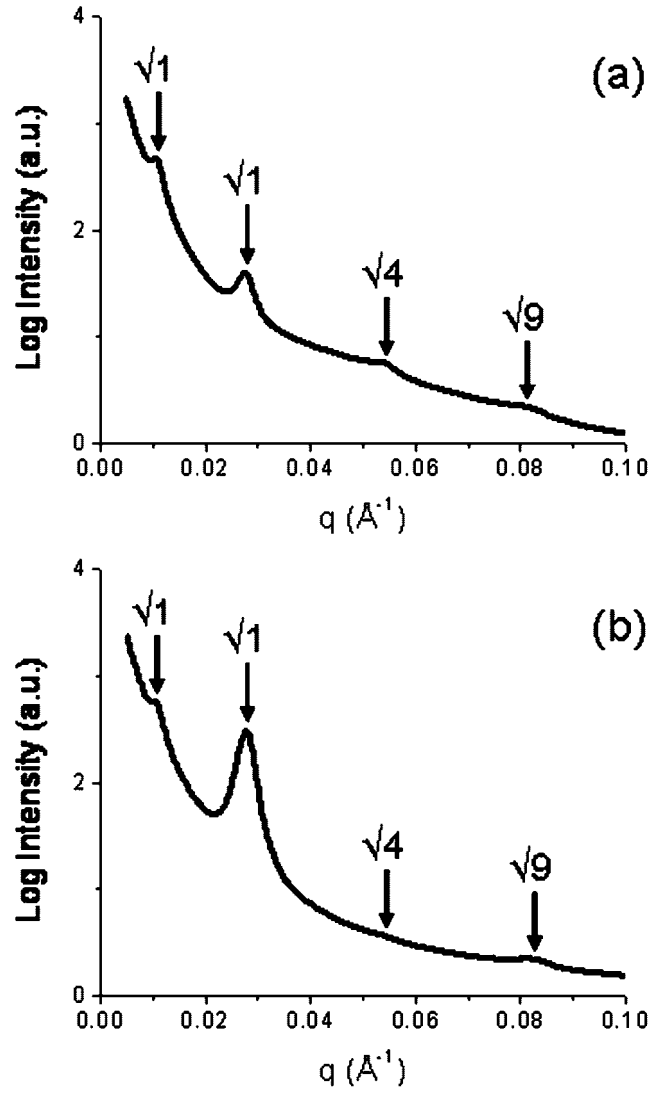

Figure 1. SAXS pattern obtained from the CECEC-P hexablock copolymer at (a) 140 °C and (b) 250 °C. The four peaks indicate two periodic structures.

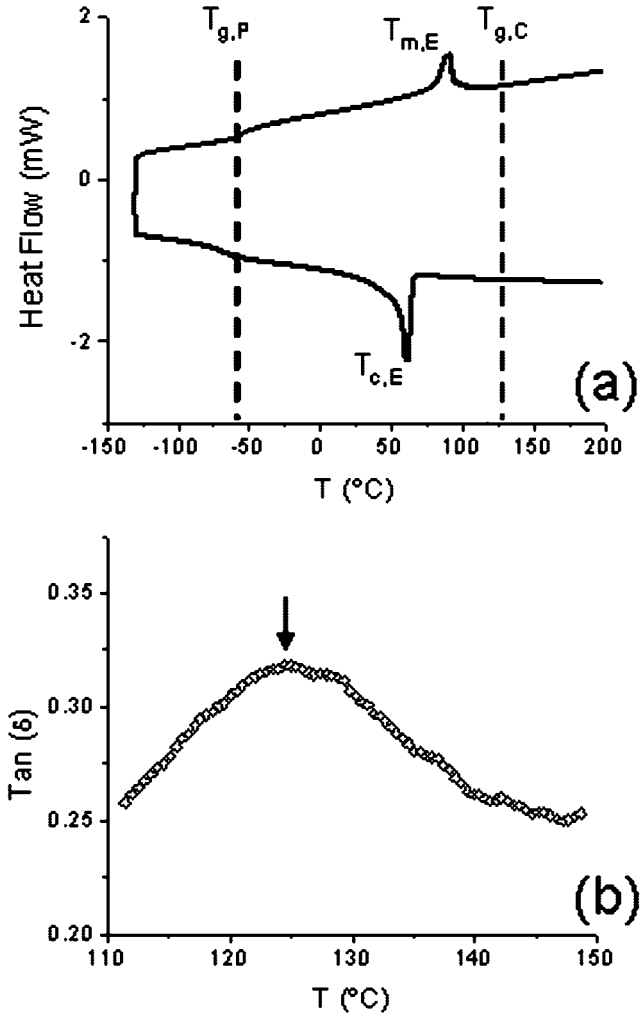

Figure 2. (a) Heating and cooling DSC traces for the CECEC-P multiblock terpolymer. The lower and upper dashed curves identify T_g for the P and C domains, respectively, while the endothermic and exothermic peaks are associated with E block melting and crystallization, respectively. (b) Isochronal dynamical measurements of tan(δ) as a function of temperature. Arrow indicates the position of the C domain glass transition identified on the DSC trace.

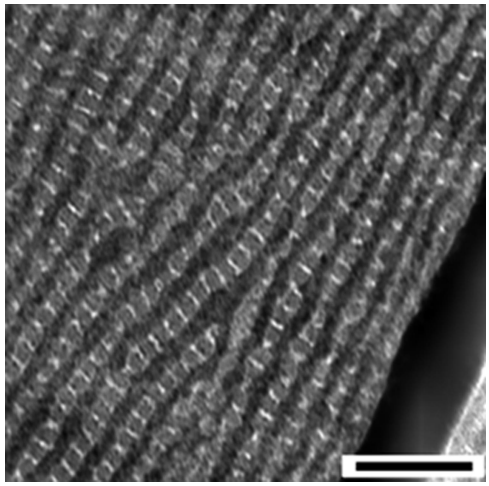

Figure 3. TEM image of RuO_4-stained CECEC-P hexablock copolymer. The darkest regions are interpreted as P domains, intermediate gray as C, and white as E. The scale bar indicates 100 nm.

fully bridging to fully looping. If confined to a three-layer sequence, the completely bridged and once looping configurations are excluded, resulting in a reduction in configurational entropy. While this argument favors the new perpendicular morphology, the chains may suffer from a different form of confinement owing to the finite width of the striped C and E microdomains. Self-consistent field theory (SCFT) calculations should be helpful in discriminating between these suggested mechanisms.

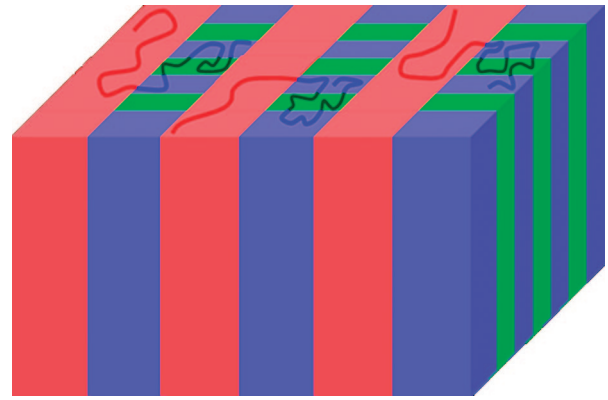

Figure 4. Lamellar-in-lamellar morphology for the CECEC-P hexablock material deduced from SAXS and TEM. Rubbery P domains (red) separate layers of semicrystalline E (green) and glassy C (blue).

We anticipate that these hexablock terpolymer materials will be characterized by interesting and potentially useful properties. On the basis of the documented behavior of bulk symmetric CECEC pentablocks, the two-dimensional layers containing C and E should be much tougher than conventional glassy domains in lamellar forming diblock and triblock copolymers. Also, the nonlinear shearing characteristics will be strongly affected by the combination of tough layers of glassy-semicrystalline polymer separated by liquid-like P domains. Experiments that probe these and other properties will be reported in a future publication.

Acknowledgment. The authors gratefully acknowledge financial support from the Department of Energy through Grant 5-35908 and the National Science Foundation (DMR-0220460). Portions of this work were carried out in the University of Minnesota Institute of Technology Characterization Facility, which receives partial support from NSF through the NNIN program and the Materials Research Science and Engineering Center (NSF-MRSEC) at the University of Minnesota (NSF DMR-0212302). Work performed at the DuPont−Northwestern−Dow Collaborative Access Team (DND-CAT) located at Sector 5 of the Advanced Photon Source (APS). DND-CAT is supported by E.I. DuPont de Nemours & Co., The Dow Chemical Company, and the State of Illinois. Use of the Advanced Photon Source (APS) was supported by the U.S. Department of Energy, Office of Science, Office of Basic Energy Sciences, under Contract DE-AC02-06CH11357.

References and Notes

(1) (a) Boncheva, M.; Whitesides, G. M. In *Dekker Encyclopedia of Nanoscience and Nanotechnology*, 2nd ed.; Schwarz, J. A., Contescu, C. I., Putyera, K., Eds.; Marcel Dekker: New York, 2004; pp 287−294. (b) Kim K. S.; Tarakeshwar, P.; Lee, H. M. In *Dekker Encyclopedia of Nanoscience and Nanotechnology*, 2nd ed.; Schwarz, J. A., Contescu, C. I., Putyera, K., Eds.; Marcel Dekker: New York, 2004; pp 2423−2433. (c) Rogers, J. A. In *Dekker Encyclopedia of Nanoscience and Nanotechnology*, 2nd ed.; Schwarz, J. A., Contescu, C. I., Putyera, K., Eds.; Marcel Dekker: New York, 2004; pp 2869−2878.
(2) Helfand, E. *Macromolecules* **1975**, *8*, 552–556.
(3) Leibler, L. *Macromolecules* **1980**, *13*, 1602–1617.
(4) Bates, F. S.; Fredrickson, G. H. *Annu. Rev. Phys. Chem.* **1990**, *41*, 525–557.
(5) Holden, G.; Legge, N. R.; Quirk, P. R.; Schroeder, H. E. In *Thermoplastic Elastomers*, 2nd ed.; Hanser Publishers: New York, 1996; pp 48−69.

(6) Quirk, R. P.; Morton, M. In *Thermoplastic Elastomers*, 2nd ed.; Hanser Publishers: New York, 1996; pp 72−100.
(7) Honeker, C. C.; Thomas, E. L. *Chem. Mater.* **1996**, *8*, 1702–1714.
(8) Bates, F. S.; Fredrickson, G. H. *Phys. Today* **1999**, *52*, 32–38.
(9) Shefelbine, T. A.; Vigild, M. E.; Matsen, M. W.; Hajduk, D. A.; Hillmyer, M. A.; Cussler, E. L.; Bates, F. S. *J. Am. Chem. Soc.* **1999**, *121*, 8457–8465.
(10) Vazaios, A.; Lohse, D. J.; Hadjichristidis, N. *Macromolecules* **2005**, *38*, 5468–5474.
(11) Stadler, R.; Auschra, C.; Beckmann, J.; Krappe, U.; Voight-Martin, I.; Leibler, L. *Macromolecules* **1995**, *28*, 4558–4561.
(12) Hirao, A.; Ryu, S. W. *Macromol. Symp.* **2003**, *192*, 31–42.
(13) Koutalas, G.; Iatrou, H.; Lohse, D. J.; Hadjichristidis, N. *Macromolecules* **2005**, *38*, 4996–5001.
(14) Weidisch, R.; Gido, S. P.; Uhrig, D.; Iatrou, H.; Mays, J.; Hadjichristidis, N. *Macromolecules* **2001**, *34*, 6333–6337.
(15) Ryu, S. W.; Asada, H.; Watanabe, T.; Hirao, A. *Macromolecules* **2004**, *37*, 6291–6298.
(16) Matsushita, Y.; Mogi, Y.; Mukai, H.; Watanabe, J.; Noda, I. *Polymer* **1994**, *35*, 246–249.
(17) Matsushita, Y.; Takasu, T.; Yagi, K.; Tomioka, K.; Noda, I. *Polymer* **1994**, *35*, 2862–2866.
(18) Lorenzo, A. T.; Alejandro J. Müller, A. J.; Priftis, D.; Pitsikalis, M.; Hadjichristidis, N. *J. Polym. Sci., Part A* **2007**, *45*, 5387–5397.
(19) Hermel, T. J.; Hahn, S. F.; Chaffin, K. A.; Gerberich, W. W.; Bates, F. S. *Macromolecules* **2003**, *36*, 2190–2193.
(20) Mahanthappa, M. K.; Lim, L. S.; Hillmyer, M. A.; Bates, F. S. *Macromolecules* **2007**, *40*, 1585–1593.
(21) Meuler, A. J.; Fleury, G.; Hillmyer, M. A.; Bates, F. S. *Macromolecules* **2008**, *41*, 5809–5917.
(22) Nagata, Y.; Masuda, J.; Noro, A.; Cho, D.; Takano, A.; Matsushita, Y. *Macromolecules* **2005**, *38*, 10220–10225.
(23) Masuda, J.; Takano, A.; Nagata, Y.; Noro, A.; Matsushita, Y. *Phys. Rev. Lett.* **2006**, *97*, 098301.
(24) Matsushita, Y. *Polym. J.* **2008**, *40*, 177–183.
(25) Masuda, J.; Takano, A.; Suzuki, J.; Nagata, Y.; Noro, A.; Hayashida, K.; Matsushita, Y. *Macromolecules* **2007**, *40*, 4023–4027.
(26) Ndoni, S.; Papadakis, C. M.; Bates, F. S.; Almdal, K. *Rev. Sci. Instrum.* **1995**, *66*, 1090–1095.
(27) Hucul, D. A.; Hahn, S. F. *Adv. Mater.* **2000**, *12*, 1855–1858.
(28) Hillmyer, M. A.; Bates, F. S. *Macromolecules* **1996**, *29*, 6994–7002.
(29) Hermel, T. J.; Hahn, S. F.; Chaffin, K. A.; Gerberich, W. W.; Bates, F. S. *Macromolecules* **2002**, *35*, 4685–4689.
(30) Khandpur, A.; Macosko, C. W.; Bates, F. S. *J. Polym. Sci., Polym. Phys.* **1995**, *33*, 247–252.
(31) Cochran, E. W.; Bates, F. S. *Macromolecules* **2002**, *35*, 7368–7374.
(32) Rosedale, J. H.; Bates, F. S.; Almdal, K.; Mortensen, K.; Wignall, G. D. *Macromolecules* **1995**, *28*, 1429–1443.
(33) Maurer, W. W.; Bates, F. S.; Lodge, T. P.; Almdal, K.; Mortensen, K.; Fredrickson, G. H. *J. Chem. Phys.* **1998**, *108*, 2989–3000.

MA900060F